

Dielectric properties and magnetostriction of the collinear multiferroic spinel CdV_2O_4

G. Giovannetti,^{1,2} A. Stroppa,³ S. Picozzi,¹ D. Baldomir,⁴ V. Pardo,⁴ S. Blanco-Canosa,⁵ F. Rivadulla,⁶ S. Jodlauk,⁷ D. Niermann,⁸ J. Rohrkamp,⁸ T. Lorenz,⁸ S. Streltsov,⁸ D. I. Khomskii,⁸ and J. Hemberger^{8,*}

¹Consiglio Nazionale delle Ricerche–SPIN, L'Aquila, Italy

²Istituto dei Sistemi Complessi–Consiglio Nazionale delle Ricerche, Dipartimento di Fisica, Università “La Sapienza”, Roma, Italy

³Consorzio Nazionale Italiano di Struttura della Materia–Dipartimento di Fisica Università degli Studi di L'Aquila, Italy

⁴Departamento de Física Aplicada, Universidad de Santiago de Compostela, 15782 Santiago de Compostela, Spain

⁵Max-Planck-Institut für Festkörperforschung, Heisenbergstrasse 1, 70569 Stuttgart, Germany

⁶Departamento Química-Física y Centro de Investigación en Química Biológica y Materiales Moleculares, Universidad de Santiago de Compostela, 15782-Santiago de Compostela, Spain

⁷Institut für Kristallographie, Universität zu Köln, Greinstr. 6, 50939 Köln, Germany

⁸II. Physikalisches Institut, Universität zu Köln, Zùlpicher Str. 77, 50937 Köln, Germany

(Received 5 November 2010; published 11 February 2011)

By studying the dielectric properties of the geometrically frustrated spinel CdV_2O_4 , we observe ferroelectricity developing at the transition into the collinear antiferromagnetic ground state. In this multiferroic spinel, ferroelectricity is driven by local exchange striction and not by the more common scenario of spiral magnetism. The experimental findings are corroborated by *ab initio* calculations of the electric polarization and the underlying spin and orbital order. The results point toward a charge rearrangement due to dimerization, where electronic correlations and the proximity to the insulator-metal transition play an important role.

DOI: [10.1103/PhysRevB.83.060402](https://doi.org/10.1103/PhysRevB.83.060402)

PACS number(s): 75.85.+t, 71.45.Gm, 71.10.Ca, 73.21.–b

Spinel form a large class of materials—probably as large as perovskites. There are many magnetic materials among them, with rich magnetic properties. In contrast to perovskites, however, there are practically no ferroelectrics in this class. Why spinels are such “bad actors” as to ferroelectricity, is actually not clear; the frustrated nature of their *B*-site sublattice can possibly play some role.¹ Only recently, the magnetically-driven ferroelectricity was found in some spinels with spiral magnetic structures, the best known example being CoCr_2O_4 ,² and there are reports of ferroelectric-like properties in ferromagnetic (FM) semiconductors HgCr_2S_4 or CdCr_2S_4 ,³ and in charge-ordered magnetite.^{4–6}

Here, we report the discovery of magnetically driven ferroelectricity in a ternary spinel with a collinear magnetic structure CdV_2O_4 . We found this multiferroic behavior experimentally, confirmed the presence of polarization, and estimated its magnitude theoretically, using *ab initio* calculations.

Vanadium spinels AV_2O_4 ($A = \text{Cd}, \text{Zn}, \text{and Mg}$) recently attracted considerable attention due to their magnetic structure and due to a possibility of orbital ordering. When decreasing the temperature, all three materials experience a structural transition from cubic to tetragonal symmetry,⁷ and at lower temperatures they also show magnetic ordering. The magnetic structure is antiferromagnetic in *ab* (or *xy*) chains, but is $\uparrow\uparrow\downarrow\downarrow$ in *xz* and *yz* chains⁸ (see Fig. 1).

Properties of related systems, with magnetic *A* sites (e.g., Mn or Fe), are similar, but the magnetic structures are more complicated. Several suggestions were proposed to explain the structural and magnetic transitions of V spinels by different types of orbital ordering. V^{3+} ions have two electrons in triply degenerate t_{2g} orbitals, which in the tetragonal phase are split into the lower occupied *xy* orbital, and doubly degenerate (*xz*, *yz*) orbitals for the remaining second electron. At least three pictures of orbital ordering of this remaining electron were suggested: alternation of *xz* and *yz* orbitals in

the *z* direction;⁹ occupation of complex orbitals $xz \pm iyz$,¹⁰ and tetramerization (occupation $xz-xz-yz-yz$ in *xz* and *yz* chains).¹¹ The description of orbital order should take into account the interplay between electron correlation, spin-orbit coupling, and cooperative Jahn-Teller distortions.¹² Recently, a different picture was suggested on the basis of *ab initio* calculations:¹³ almost no orbital ordering of this second electron, but strong alternation of V–V distances in the *xz* and *yz* directions, with FM bonds becoming shorter.

The magnetic structure, with $\uparrow\uparrow\downarrow\downarrow$ spin ordering along a chain, is reminiscent of the situation in *E*-type manganites such as HoMnO_3 ,^{14,15} and in $\text{Ca}_3\text{CoMnO}_6$,¹⁶ which are both multiferroic. This would suggest that multiferroicity can be found in V spinels as well. This is indeed confirmed by our experimental and theoretical study.

The single-phase, polycrystalline samples of CdV_2O_4 were prepared by a solid-state reaction in evacuated quartz ampoules, as described in Ref. 17. Simultaneously, also, the samples of ZnV_2O_4 and MgV_2O_4 were synthesized. Structural and magnetic measurements confirmed the known behavior: In our samples of CdV_2O_4 a cubic-tetragonal transition occurs at $T_S \approx 95$ K, and at $T_N \approx 33$ K there appears antiferromagnetic ordering. Both transitions cause pronounced anomalies in the thermal expansion coefficient $\alpha(T)$, measured in a home-built capacitance dilatometer [see Fig. 2(a)]. The measurements of electric polarization were made in a conventional ^4He -flow magnetocryostat (Oxford) by evaluating the integrated pyrocurrent recorded with a high-precision electrometer. Also, the complex, frequency-dependent dielectric response was measured by employing a frequency-response analyzer (Novocontrol) with pseudo-four-point probing for the linear measurements under small stimulus and with two-point probing for the nonlinear measurements in electric driving fields up to 220 V_{rms} . For both purposes, silver paint contacts were applied to the platelike polycrystalline

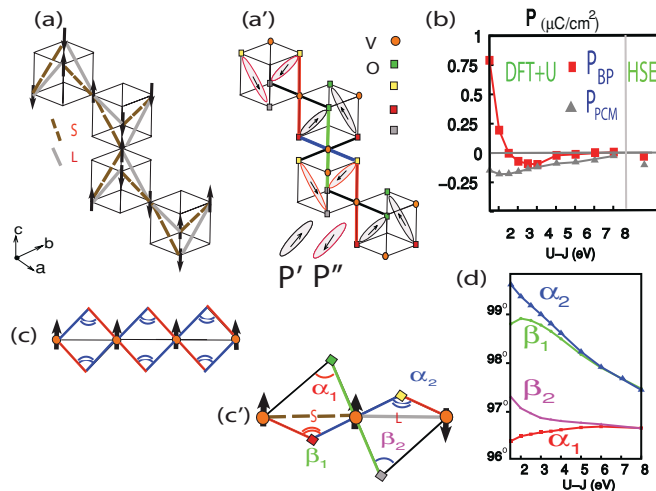


FIG. 1. (Color online) Schematic view of (a) the V-O ionic arrangements with spin magnetic structure (see black arrows) and short (long) V-V bond lengths highlighted by dashed (bold solid) lines; (a') oxygen-induced dipoles (see ellipses) and long bond-length V-O (see black lines)—symmetry inequivalent oxygens are denoted with different symbols/colors; (b) calculated polarization according to DFT+ U (left) and HSE schemes (right); V and O arrangement for (c) $\uparrow\uparrow\uparrow\uparrow$ and (c') $\uparrow\uparrow\downarrow\downarrow$ spin ordering along $[101]$ or $[011]$; (d) values of α_1 , β_2 , α_2 , and β_1 angles as a function of U_{eff} .

pellets in sandwich geometry with a typical electrode area of $A \approx 10 \text{ mm}^2$ and a thickness of $d \approx 1 \text{ mm}$. The uncertainty in the determination of the exact geometry, together with additional (but constant) contributions of stray capacitances in two-point probing, results in an uncertainty in the absolute values for electric polarization and permittivity of up to 20%.

Results of the dielectric measurements are shown in Figs. 2 and 3. The dielectric permittivity displays a small anomaly at the structural transition temperature $T_S \approx 95 \text{ K}$ [Fig. 2(b2)] and a sharp jumplike anomaly at the magnetic transition $T_N \approx 33 \text{ K}$. The latter slightly depends on an external magnetic field as demonstrated by the data for zero field and 10 T displayed in Fig. 2(b1): The anomaly shifts slightly to lower temperatures under applying a magnetic field. At the same time, the permittivity possesses a distinct frequency-dependent contribution superimposed on the described features: A step in $\epsilon'(T)$ is accompanied by a peak in $\epsilon''(T)$ shifting to lower temperatures with decreasing frequency. A very similar relaxational contribution along the c axis was found in multiferroic rare earth manganites. There, it was ascribed either to the freezing of an overdamped polar lattice mode or, alternatively, one could think of the relaxation of localized polarons at defect states.¹⁸ In any case, these data demonstrate that the dielectric properties are to some extent influenced by the experimental time window.

That the sharp dielectric anomaly at T_N is connected with the onset of spontaneous electric polarization is demonstrated in Fig. 3(a), which displays the electric polarization $P(T)$. The difference between the cooling data detected in the presence of an electric poling field, compared to the zero-field heating data, may be explained by field-induced contributions such as reversible domain orientation or the aforementioned relaxational contribution. The latter can be noticed as a

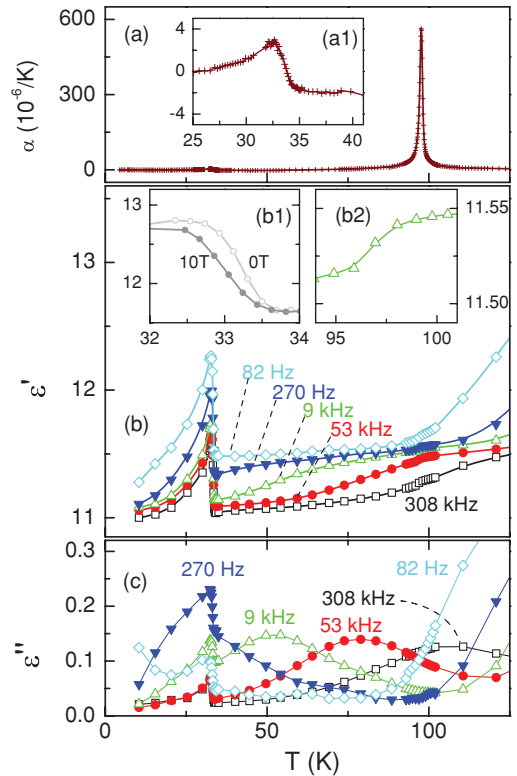


FIG. 2. (Color online) Thermal expansion α in the whole temperature range (a) and in the vicinity of the magnetic transition (a1). The complex dielectric permittivity ϵ^* of CdV_2O_4 is displayed as real part ϵ' (b) and as dielectric loss ϵ'' (c) for different frequencies between 82 Hz and 0.3 MHz measured with a stimulus of $\sim 1 \text{ V/mm}$. The data displayed in frame (b1) were measured in the vicinity of the magnetic transition at 1 Hz in external fields of zero and 10 T. Frame (b2) shows the small dielectric anomaly at the structural transition below 100 K.

broad loss peak in $\epsilon''(T)$ above 10 K in the plot of the linear component of the complex permittivity, which was measured with a large stimulating electric field and is displayed in Fig. 3(b). The behavior of the nonlinear component of the permittivity ϵ_{nl} evaluated from the third harmonic of the dielectric response can be taken as additional evidence for the onset of ferroelectricity [Fig. 3(c)]. The onset of the third-order nonlinearity is followed by a decay toward lower temperatures that is related to the increase of the coercivity: For temperatures below 25 K, the driving field of $220 \text{ V}_{\text{rms}}/\text{mm}$ cannot switch ferroelectric domains anymore. It has to be noted that the second harmonic contribution (not shown) stays within the harmonic distortion of the setup at T_N , as expected for a symmetric polarization response $M(H)$.

All of these data unequivocally demonstrate that there appears spontaneous polarization in CdV_2O_4 below T_N . The magnitude of polarization obtained in our samples [Fig. 3(a)] is $P \approx 5 \mu\text{C}/\text{m}^2$. One should expect that in a single-domain single crystal the polarization should be much larger. Similar measurements on polycrystals of ZnV_2O_4 and MgV_2O_4 did not show ferroelectric behavior: Polarization is absent (within the accuracy of $P < 0.1 \mu\text{C}/\text{m}^2$). We discuss possible reasons for such a different behavior in the following.

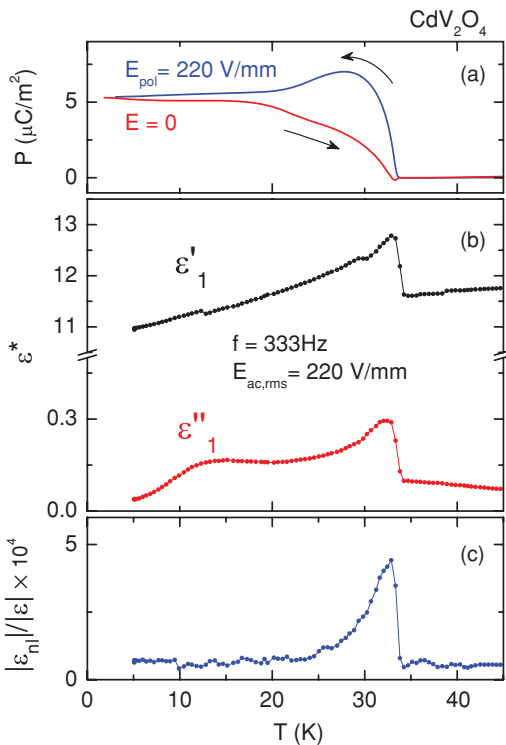


FIG. 3. (Color online) Electric polarization (a) measured via the pyrocurrent under cooling with a rate of 2 K/min in an electric poling field of 220 V/mm and under heating with the same rate in zero external field. Frame (b) displays the linear component of the dielectric permittivity measured with a stimulus of 220 V_{rms}/mm. The corresponding (third-order) nonlinear component $|\epsilon_{nl}|$ normalized on the linear term is displayed in (c); the “floor” of roughly 0.8×10^{-4} can be attributed to the harmonic distortion of the high-voltage amplifier.

The explanation of the appearance of polarization in CdV₂O₄ has some analogy with the mechanism proposed for *E*-type manganites.^{14,19} The distortion, in particular the shifts of oxygens, is different in the vicinity of FM and antiferromagnetic bonds. The main feature of the corresponding lattice distortions is the dimerization of V-V bonds,¹³ but the shifts of the oxygens are also present, which ultimately leads to polarization. A specific feature of spinels (i.e., the existence of *two* oxygens “attached” to each V-V bond, compared to *one* oxygen in *E*-type manganites) makes the picture more complicated, but the main physical mechanism is very similar.

In order to shed light on the origin of the ferroelectricity, we performed *ab initio* calculations using the projector augmented-wave (PAW) method²⁰ with plane-wave basis sets as implemented in the Vienna *ab initio* simulation package (VASP).²¹ To describe the correlation effects of V-3*d* electrons, we used the density functional theory using the Hubbard-*U* correction (DFT + *U*),²² for different values of $U_{\text{eff}} = U - J_H$ ranging between 0 and 8 eV, and the Heyd-Scuseria-Ernzerhof (HSE) hybrid functional.²³ The HSE has been shown to provide accurate treatments of solid state systems in which the delicate balance between itinerancy and localization plays an important role.²⁴ Furthermore, HSE does not require system-dependent adjustable parameters or decisions of which electrons to localize,²⁵ and it can provide a benchmark calculation for the DFT + *U* method. We therefore expect that

HSE is well suited for systems in which *partial delocalization effects* are at play, as in the system under study.¹³ The DFT + *U* formalism leads to results comparable to those obtained by means of HSE, provided that the value of the *U* parameter is adequately chosen.

Starting from the tetragonal experimental crystal structure with $I4_1/amd$ centric symmetry,²⁶ we performed ionic relaxations for different values of U_{eff} , keeping the V magnetic moments ordered as $\uparrow\uparrow\downarrow\downarrow$ along the [101] and [011] directions [see Fig. 1(a)]. The relaxed structure shows the formation of short (S) and long (L) bonds between $\uparrow\uparrow$ and $\uparrow\downarrow$ moments, respectively; cf. also Refs. 13 and 27. For large values of U_{eff} , the general trend toward formation of V-V dimers is reduced. (Note that, by imposing the FM spin ordering, the structure retains the inversion symmetry, and no dimerization is found for any values of U_{eff} .) Further inspection of the relaxed polar ionic structures shows that the spin, orbital, and lattice degrees of freedom are coupled: In plane *xz*, *yz* long bonds are oriented as reminiscent of a Kugel-Khomskii model²⁸ and of the experimental structure proposed for ZnV₂O₄ (Ref. 29) [see Fig. 1(a)]. For the relaxed structure, we evaluated the ferroelectric polarization P_{BP} [see Fig. 1(b)] according to the Berry phase (BP) theory.³⁰ We obtained a finite P_{BP} , directed along the *c* axis, that is strongly related to the formation of a dimerized structure at intermediate values of U_{eff} . The electronic charge redistribution due to dimer formation gives rise to differences between the BP and the point charge model (PCM) values of P . The red curve in Fig. 1(b) is the total polarization, ionic plus electronic (BP) contribution (i.e., P_{BP}); the gray curve is the estimate of the point charge model (using the ionic nominal valencies). The fact that they are different suggests that covalency effects are relevant.

We now discuss the mechanism behind ferroelectricity. First of all, let us recall that if we consider a FM ($\uparrow\uparrow\uparrow\uparrow$) state with the suggested experimental $I4_1/amd$ symmetry,²⁶ all V-O-V angles are equivalent along the chain [see Fig. 1(c)]. Note, however, that V-O distances are slightly different, due to the peculiar coordination of the spinel structure: Each O is an “apical” one with respect to one V ion and a “planar” one with respect to the other neighboring V ion. This does not exclude *a priori* some degree of orbital ordering, even in a FM spin configuration. As expected from the centrosymmetric space group, no polarization is found from our calculations for this case. However, once the magnetic order $\uparrow\uparrow\downarrow\downarrow$ is imposed, (i) the angles α_1 and β_2 (α_2 and β_1) become inequivalent as a consequence of the formation of short and long V-V bonds; (ii) α_1 and β_1 become different. The long V-O bonds are arranged as shown in Fig. 1(a). This pattern is compatible with a weakly staggered *xz*, *yz* orbital ordering. As a result, the dipole moments P' and P'' , originating from the inequivalency of oxygens, and schematically shown in Fig. 1(a'), appear due to different α_1 and β_2 (α_2 and β_1) angles; since P' and P'' do not compensate, they give rise to a net P . This picture is valid for intermediate values of U_{eff} . At large values of U_{eff} , however, the inequivalency of α_1 and β_2 (α_2 and β_1) V-O-V angles disappears [see point (i) above, whereas (ii) is still valid] [see Fig. 1(d)]; as a result, P is suppressed, but is still nonzero. In other words, the $\uparrow\uparrow\downarrow\downarrow$ spin ordering, imposed onto the centric $I4_1/amd$ space group, gives rise to an *electronic instability* that ultimately

results in a V-V dimerization *and* formation of short and long V-O bonds, compatible with a staggered xz, yz orbital ordering. This electronic instability is already evident *before* ionic optimization: the two \uparrow (\downarrow) V sites are inequivalent by symmetry, and, upon ionic relaxations, this inequivalency eventually drives the V-V dimerization. Also the two oxygens bonded to \uparrow, \uparrow V (or \downarrow, \downarrow V) become inequivalent, in turn giving rise, upon ionic relaxations, to a weakly staggered orbital ordering. Both effects cooperate to stabilize the polarization.

Thus the theoretical results confirm, first of all, the structure proposed in Ref. 13, with dimerization in V-V chains in xz and yz directions. Furthermore, they show that CdV_2O_4 is ferroelectric. The calculated polarization is along the c direction, and its value is $P \approx 200 \mu\text{C}/\text{m}^2$. This is typical for multiferroics with ferroelectricity induced by magnetic exchange striction, such as HoMnO_3 or YMn_2O_5 (see, e.g., Ref. 15). The fact that the experimentally observed value is smaller, $P \approx 5 \mu\text{C}/\text{m}^2$, as mentioned earlier, is rather common. The same happens in HoMnO_3 : The measured value in polycrystalline material $P \approx 90 \mu\text{C}/\text{m}^2$ ¹⁵ is smaller than the theoretical value¹⁴—which, however, agrees with the estimates obtained from optical studies.³¹ Most likely it is connected with the polycrystalline nature of the samples: First, polarization is averaged over all directions, but most important is that probably in these granular materials one does not reach full domain orientation during the poling procedure used.

Why the polarization is absent in the measured samples of ZnV_2O_4 and MgV_2O_4 , is not completely clear. Theoretically

we could expect that these spinels, with very similar structure, could also be multiferroic. One of the reasons could be that these materials have much smaller gaps than CdV_2O_4 (Ref. 13) and are close to the localized-itinerant crossover.¹⁷ The finite conductivity of these samples [10^4 times higher than in CdV_2O_4 (Ref. 13)] may scramble the results of the measurements. The quality of the samples may also matter. In any case, this question deserves further study.

Summarizing, we discovered a multiferroic ternary spinel with collinear magnetic structure, CdV_2O_4 . We thus showed that not only a spiral magnetic structure can produce ferroelectricity in spinels; the exchange striction mechanism can do it as well. In the latter case, polarization is usually larger than in spiral magnets, which is also the case here.

Our study also clarifies the question about orbital ordering and structural distortions in V spinels, confirming that there should appear a strong V-V dimerization, that is also responsible for polarization. We conclude by suggesting that similar phenomena might occur in other spinels, thus broadening the class of multiferroic systems to this group of materials.

The research leading to the *ab initio* results has received funding from the European Research Council under the EU 7th Framework Programme (FP7/2007-2013)/ERC Grant Agreement No. 203523 and through programs MK-360.2009.2, MAT2009-08165 and INCITE08PXIB236052PR. The experimental work has been funded by the Deutsche Forschungsgemeinschaft (DFG) through SFB608 (Cologne).

*Corresponding author: hemberger@ph2.uni-koeln.de

¹R. Seshadri, *Solid State Sci.* **8**, 259 (2006).

²Y. Yamasaki, S. Miyasaka, Y. Kaneko, J.-P. He, T. Arima, and Y. Tokura, *Phys. Rev. Lett.* **96**, 207204 (2006).

³J. Hemberger *et al.*, *Nature (London)* **434**, 364 (2005); S. Weber, P. Lunkenheimer, R. Fichtl, J. Hemberger, V. Tsurkan, and A. Loidl, *Phys. Rev. Lett.* **96**, 157202 (2006).

⁴M. Alexe *et al.*, *Adv. Mater.* **21**, 4452 (2009).

⁵J. van den Brink and D. I. Khomskii, *J. Phys.: Condens. Matter* **20**, 434217 (2008).

⁶K. Yamauchi, T. Fukushima, and S. Picozzi, *Phys. Rev. B* **79**, 212404 (2009).

⁷Y. Yamashita and K. Ueda, *Phys. Rev. Lett.* **85**, 4960 (2000); Z. Zhang, D. Louca, A. Visinoiu, S.-H. Lee, J. D. Thompson, T. Proffen, A. Llobet, Y. Qiu, S. Park, and Y. Ueda, *Phys. Rev. B* **74**, 014108 (2006).

⁸M. Reehuis *et al.*, *Eur. Phys. J. B* **35**, 311 (2003).

⁹Y. Motome and H. Tsunetsugu, *Phys. Rev. B* **70**, 184427 (2004).

¹⁰O. Tchernyshyov, *Phys. Rev. Lett.* **93**, 157206 (2004).

¹¹D. I. Khomskii and T. Mizokawa, *Phys. Rev. Lett.* **94**, 156402 (2005).

¹²S. Sarkar, T. Maitra, R. Valenti, and T. Saha-Dasgupta, *Phys. Rev. Lett.* **102**, 216405 (2009); T. Maitra and R. Valenti, *ibid.* **99**, 126401 (2007).

¹³V. Pardo, S. Blanco-Canosa, F. Rivadulla, D. I. Khomskii, D. Baldomir, H. Wu, and J. Rivas, *Phys. Rev. Lett.* **101**, 256403 (2008).

¹⁴S. Picozzi, K. Yamauchi, B. Sanyal, I. A. Sergienko, and E. Dagotto, *Phys. Rev. Lett.* **99**, 227201 (2007).

¹⁵B. Lorenz, Y. Q. Wang, and C. W. Chu, *Phys. Rev. B* **76**, 104405 (2007).

¹⁶Y. J. Choi, H. T. Yi, S. Lee, Q. Huang, V. Kiryukhin, and S.-W. Cheong, *Phys. Rev. Lett.* **100**, 047601 (2008).

¹⁷S. Blanco-Canosa *et al.*, *Phys. Rev. Lett.* **99**, 187201 (2007).

¹⁸F. Schrettle, P. Lunkenheimer, J. Hemberger, V. Yu. Ivanov, A. A. Mukhin, A. M. Balbashov, and A. Loidl, *Phys. Rev. Lett.* **102**, 207208 (2009).

¹⁹S. Picozzi and C. Ederer, *J. Phys.: Condens. Matter* **21**, 303201 (2009).

²⁰P. E. Blöchl, *Phys. Rev. B* **50**, 17953 (1994).

²¹G. Kresse and J. Furthmüller, *Phys. Rev. B* **54**, 11169 (1996); *Comput. Mater. Sci.* **6**, 15 (1996).

²²S. L. Dudarev, G. A. Botton, S. Y. Savrasov, C. J. Humphreys, and A. P. Sutton, *Phys. Rev. B* **57**, 1505 (1998).

²³J. Heyd *et al.*, *J. Chem. Phys.* **118**, 8207 (2003).

²⁴P. J. Hay *et al.*, *J. Chem. Phys.* **125**, 034712 (2006).

²⁵M. Marsman *et al.*, *J. Phys.: Condens. Matter* **20**, 064201 (2008); A. Stroppa and G. Kresse, *Phys. Rev. B* **79**, 201201(R) (2009); A. Stroppa *et al.*, *PhysChemChemPhys* **12**, 5405 (2010).

²⁶M. Onoda *et al.*, *J. Phys.: Condens. Matter* **15**, L95 (2003).

²⁷E. M. Wheeler, B. Lake, A. T. M. Nazmul Islam, M. Reehuis, P. Steffens, T. Guidi, and A. H. Hill, *Phys. Rev. B* **82**, 140406(R) (2010).

²⁸K. I. Kugel and D. I. Khomskii, *Zh. Eksp. Teor. Fiz.* **64**, 1429 (1973) [*Sov. Phys. JETP* **37**, 725 (1973)].

²⁹S.-H. Lee *et al.*, *Phys. Rev. Lett.* **93**, 156407 (2004).

³⁰R. D. King-Smith and D. Vanderbilt, *Phys. Rev. B* **47**, 1651 (1993); D. Vanderbilt and R. D. King-Smith, *ibid.* **48**, 4442 (1993).

³¹R. Valdés Aguilar, M. Mostovoy, A. B. Sushkov, C. L. Zhang, Y. J. Choi, S.-W. Cheong, and H. D. Drew, *Phys. Rev. Lett.* **102**, 047203 (2009).